The EMBO Journal (2006) 25, 4423–4435 | © 2006 European Molecular Biology Organization | All Rights Reserved 0261-4189/06
www.embojournal.org

THE EMBO JOURNAL

A PACS-1, GGA3 and CK2 complex regulates CI-MPR trafficking

Gregory K Scott, Hao Fei[1], Laurel Thomas, Guruprasad R Medigeshi[2] and Gary Thomas*

Vollum Institute, Portland, OR, USA

The cation-independent mannose-6-phosphate receptor (CI-MPR) follows a highly regulated sorting itinerary to deliver hydrolases from the *trans*-Golgi network (TGN) to lysosomes. Cycling of CI-MPR between the TGN and early endosomes is mediated by GGA3, which directs TGN export, and PACS-1, which directs endosome-to-TGN retrieval. Despite executing opposing sorting steps, GGA3 and PACS-1 bind to an overlapping CI-MPR trafficking motif and their sorting activity is controlled by the CK2 phosphorylation of their respective autoregulatory domains. However, how CK2 coordinates these opposing roles is unknown. We report a CK2-activated phosphorylation cascade controlling PACS-1- and GGA3-mediated CI-MPR sorting. PACS-1 links GGA3 to CK2, forming a multimeric complex required for CI-MPR sorting. PACS-1-bound CK2 stimulates GGA3 phosphorylation, releasing GGA3 from CI-MPR and early endosomes. Bound CK2 also phosphorylates PACS-1Ser$_{278}$, promoting binding of PACS-1 to CI-MPR to retrieve the receptor to the TGN. Our results identify a CK2-controlled cascade regulating hydrolase trafficking and sorting of itinerant proteins in the TGN/endosomal system.

The EMBO Journal (2006) **25,** 4423–4435. doi:10.1038/sj.emboj.7601336; Published online 14 September 2006
Subject Categories: membranes & transport
Keywords: CI-MPR; CK2; endosome; GGA3; PACS-1

Introduction

The localization and trafficking of itinerant membrane cargo proteins within the *trans*-Golgi network (TGN)/endosomal system relies upon canonical sorting motifs within their cytosolic domains, which are recognized by components of the vesicular trafficking machinery (Robinson, 2004). These motifs include tyrosine (Yxxϕ)- and dileucine ([D/E]xxxL[L/I])-based signals, which bind to the heterotetrameric adaptors (APs), acidic-dileucine (DxxLL)-based motifs, which bind to GGAs and acidic cluster-based motifs, which bind to PACS proteins. The cytosolic domain of one membrane protein, the cation-independent mannose-6-phosphate receptor (CI-MPR), requires motifs that bind to each of these three groups of sorting molecules to localize to the TGN and to efficiently sort cathepsin D to lysosomes (Chen *et al*, 1997; Wan *et al*, 1998; Meyer *et al*, 2000; Puertollano *et al*, 2001a; Ghosh *et al*, 2003). The GGAs sort the CI-MPR into clathrin-coated vesicles at the TGN and may also mediate CI-MPR trafficking between endosomal compartments (Doray *et al*, 2002b; Mattera *et al*, 2003; Puertollano and Bonifacino, 2004). By contrast, PACS-1 and AP-1, which mediate endosome-to-TGN retrieval, are required to localize CI-MPR to the TGN (Wan *et al*, 1998; Meyer *et al*, 2000; Crump *et al*, 2001). In addition, other sorting molecules including TIP47, Retromer and EpsinR also function in the endosome-to-TGN retrieval of CI-MPR (Diaz and Pfeffer, 1998; Arighi *et al*, 2004; Saint-Pol *et al*, 2004; Seaman, 2004), supporting the highly regulated and complex trafficking pathway followed by this multifunctional receptor.

We identified PACS-1 through its binding to the protein kinase CK2 (CK2)-phosphorylated acidic cluster (…EECPpSDpSEEDE…) on the furin cytosolic domain (Figure 1A and Wan *et al*, 1998). The 140 amino acid PACS-1 cargo-binding region (FBR, Figure 1A) contains an eight-amino-acid segment ETELQLTF$_{175}$ that binds AP-1, and is required for correct subcellular localization of furin and CI-MPR to the TGN (Crump *et al*, 2001). PACS-1 also binds to acidic cluster motifs on several additional itinerant cellular proteins (Thomas, 2002), including proprotein convertase 6B (Xiang *et al*, 2000), polycystin-2 (Köttgen *et al*, 2005) and VAMP4 (Hinners *et al*, 2003), as well as the viral proteins HCMV gB (Crump *et al*, 2003) and HIV-1 Nef (Piguet *et al*, 2000). Studies using dominant negative-, siRNA- or antisense-based methods show PACS-1 is required for the TGN localization of each of these proteins, suggesting a broad role for PACS-1 in cellular homeostasis and disease.

Similar to furin, binding of PACS-1 to the CI-MPR cytosolic domain (CI-MPR$_{CD}$) requires the CK2 phosphorylatable acidic cluster …DDpSDEDLLHI, located at the CI-MPR$_{CD}$ C-terminus (Wan *et al*, 1998). Interestingly, the three GGA family members (1–3) also bind to this phosphorylated motif on the CI-MPR$_{CD}$ but require the dileucine motif for binding, which furin lacks (Puertollano *et al*, 2001a). The GGAs contain three principal domains including the VHS domain, which binds to cargo proteins, the GAT domain, which binds to ARF1, a hinge segment, which binds clathrin and contains an autoregulatory acidic-dileucine motif (GGA1 and 3 only) and the GAE domain, which binds to several accessory proteins (Figure 1B and Bonifacino, 2004). Through these interactions, the GGAs function as monomeric clathrin adaptors that link itinerant cargo directly to clathrin (Puertollano *et al*, 2001b). However, why GGAs and PACS-1 share overlapping binding sites on the CI-MPR$_{CD}$ is not known.

The functional similarities shared by PACS-1 and GGAs extend to regulation of their cargo binding. The sorting

*Corresponding author. Vollum Institute, Oregon Health & Science University, Oregon Health Sciences University, L-474, 3181 SW Sam Jackson Park Road, Portland, OR 97239-3098, 97239, USA.
Tel.: +1 503 494 6955; Fax: +1 503 494 1218;
E-mail: thomasg@ohsu.edu
[1]Present address: Department of Psychiatry and Biobehavioral Sciences, UCLA, Los Angeles, CA 90095, USA
[2]Present address: Department of Molecular Microbiology and Immunology, OHSU, Portland, OR, USA

Received: 10 January 2006; accepted: 16 August 2006; published online: 14 September 2006

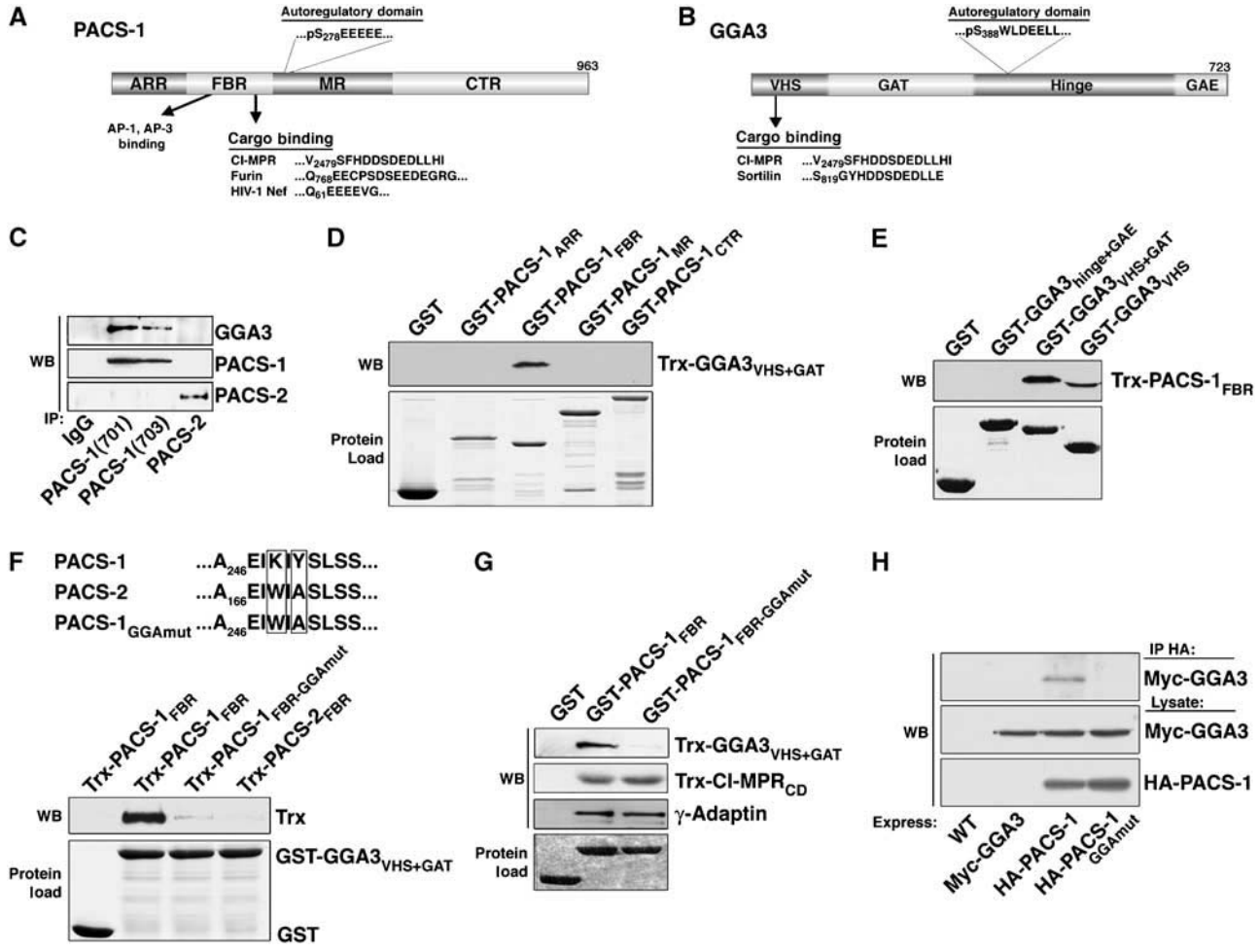

Figure 1 PACS-1 binds to GGA3. (**A**) Diagram of PACS-1 showing the atropin-1-related region (ARR), cargo-binding region (FBR), which interacts with cargo and AP-1/AP-3 adaptor complexes (Wan *et al*, 1998; Crump *et al*, 2001), the middle region (MR), which contains the autoregulatory acidic cluster and Ser_{278} (Scott *et al*, 2003), and the C-terminal region (CTR) and PACS-1 cargo. (**B**) Diagram of GGA3 showing the VHS (Vps27, Hrs, Stam) domain, which binds to cargo proteins, the GAT (GGA and TOM) domain, which binds to ARF1, the hinge segment, which contains the autoregulatory acidic-dileucine motif and Ser_{388}, and the GAE (γ-adaptin ear) domain (Bonifacino, 2004) and GGA3 cargo. (**C**) Endogenous PACS-1 was immunoprecipitated from rat brain (lower panel) using anti-PACS-1 701 or 703, anti-PACS-2 834 or control IgG and co-precipitating GGA3 analyzed by SDS–PAGE and Western blot (upper panel). Immunoprecipitated PACS-1 and PACS-2 are shown by Western blot (bottom panel). (**D–G**) The indicated GST-fusion proteins were incubated with the indicated Trx-fusion proteins or with purified AP-1, isolated with glutathione sepharose and analyzed by Western blot using anti-Trx or anti-γ-adaptin antibody (upper panels). Each GST-protein is also shown (lower panel). The Trx-PACS-1_{FBR} (residues 117–294) band is shifted lower in (E) because Trx-PACS-1_{FBR} migrates at the same size as GST-$GGA3_{VHS}$. GST-$GGA3_{VHS-GAT}$ captured ~1% of Trx-PACS-1_{FBR} input, and GST-PACS-1_{FBR} (residues 117–294) captured ~1%, 0.5% and 1% of the Trx-$GGA3_{VHS-GAT}$, γ-adaptin and Trx-CI-MPR_{cd} input, respectively. Binding assays were conducted as described in Materials and methods, except 4% NP40 was used. (**H**) A7 cells infected with wild-type (WT) AV or AV expressing Myc-GGA3, Myc-GGA3 and HA-PACS-1, or Myc-GGA3 and HA-PACS-1_{GGAmut} were harvested and HA-tagged proteins immunoprecipitated and co-precipitating myc-GGA analyzed by Western blot (upper panel). Lower panels show myc-GGA3 and HA-PACS-1 expression.

activity of PACS-1 is regulated by the CK2- and PP2A-controlled phosphorylation of an autoregulatory domain (Scott *et al*, 2003). Phosphorylation of PACS-$1Ser_{278}$ within the PACS-1 autoregulatory domain activates cargo binding and is required for the endosome-to-TGN transport of furin, CI-MPR and HIV-1 Nef. Similar to PACS-1, GGA1 and GGA3 binding to cargo proteins is regulated by CK2 phosphorylation of an autoregulatory domain within the GGA1 and GGA3 hinge segment (Doray *et al*, 2002a; Ghosh and Kornfeld, 2003). Phosphorylation of $GGA1Ser_{355}$ (which corresponds to $GGA3Ser_{388}$, see Figure 1B) within the GGA1 autoregulatory domain inhibits binding to CI-MPR. Therefore, CK2 phosphorylation of the PACS-1 autoregulatory domain *promotes* cargo binding (Scott *et al*, 2003), whereas CK2 phosphorylation of GGA1 or three autoregulatory domains *inhibits* cargo binding (Doray *et al*, 2002a).

CK2 is a ubiquitous protein kinase with more than 300 putative polypeptide substrates and is a heterotetramer composed of two catalytic subunits (αα, αα′, or α′α′) and two regulatory β subunits (Meggio and Pinna, 2003). The regulation of this basally active kinase has long remained enigmatic, although the binding of the regulatory β subunit to polyamines or substrate proteins can increase kinase activity three-fold (Litchfield, 2003). The requirement for CK2 phosphorylation for the regulation of PACS-1, GGA1 and GGA3 action led us to determine how this kinase may control the

PACS-1 and GGA3-mediated trafficking of CI-MPR. We report that PACS-1 binds to GGA3 and recruits CK2, forming a multimeric complex, which regulates PACS-1/GGA3-mediated sorting of CI-MPR between the TGN and early endosomes. Together our results describe a novel cellular mechanism for the phospho-regulation of membrane protein traffic through the TGN/endosomal system.

Results

PACS-1 binds to GGA3

Despite regulating opposing CI-MPR trafficking steps, PACS-1 and GGAs share several biochemical functions. These include binding to the CI-MPR$_{CD}$ at a C-terminal acidic cluster and the regulation of their binding to membrane cargo by the CK2 phosphorylation of an autoregulatory domain (Wan *et al*, 1998; Puertollano *et al*, 2001a; Doray *et al*, 2002a; Scott *et al*, 2003). These common properties led us to ask if GGA3 and PACS-1 associate *in vivo*. Accordingly, we immunoprecipitated PACS-1 from rat brain using two different PACS-1 antibodies and found that GGA3 co-precipitated with PACS-1 (Figure 1C). By contrast, GGA3 did not co-precipitate with PACS-2, which is a PACS-1 homologue that mediates ER/mitochondria trafficking (Simmen *et al*, 2005). To determine if PACS-1 bound directly to GGA3 and to identify the GGA3-binding region of PACS-1, we used glutathione-*S*-transferase (GST)-tagged PACS-1 fusion proteins corresponding to predicted domains of PACS-1 (Figure 1A) to capture Thioredoxin (Trx)-tagged GGA3$_{VHS+GAT}$ (Figure 1D). Only GST-PACS-1$_{FBR}$, which binds to cargo including CI-MPR$_{CD}$, was able to precipitate Trx-GGA3$_{VHS+GAT}$. Reciprocal mapping experiments using purified GST-GGA3 constructs (Figure 1B) showed that the GGA3 VHS domain, which binds the CI-MPR$_{CD}$, was sufficient to bind Trx-PACS-1$_{FBR}$ (Figure 1E). These results demonstrate a direct interaction between PACS-1 and GGA3 through their cargo-binding regions.

To further define the GGA3-binding site on the PACS-1 FBR, we took advantage of the fact that through the FBR, PACS-1 and PACS-2 are 75% identical and 83% homologous. Serial mutation of nonhomologous amino acids was used to identify residues in the PACS-1 FBR required for binding GGA3. Using this approach, we found that mutation of PACS-1 FBR residues K$_{249}$IY to the corresponding PACS-2 residues (W$_{171}$IA; hereafter PACS-1 FBR-GGAmut) disrupted GGA3 binding (Figure 1F). In addition, we found that protein-binding studies showed that the K$_{249}$Y$_{251}$→WA substitution had no effect on GST-PACS-1$_{FBR}$ binding to purified AP-1 or Trx-tagged CI-MPR$_{CD}$ (Figure 1G). Therefore, we introduced the K$_{249}$Y$_{251}$→WA mutation into full-length PACS-1 (hereafter PACS-1$_{GGAmut}$), and compared the ability of hemagglutinin (HA)-tagged PACS-1 and HA-PACS-1$_{GGAmut}$ to co-immunoprecipitate co-expressed myc-GGA3 (Figure 1H). In agreement with our *in vitro* binding studies, we found that myc-GGA3 co-immunoprecipitated with HA-PACS-1, but not with HA-PACS-1$_{GGAmut}$. Thus, we identified a PACS-1 mutant that fails to bind GGA3 but is unaffected for binding cargo and AP-1.

Blocking the PACS-1/GGA3 interaction disrupts CI-MPR and GGA3 localization

We expressed PACS-1$_{GGAmut}$ in cells to determine if PACS-1 binding to GGA3 is required for the steady-state localization of their mutual cargo protein: CI-MPR. In control cells or PACS-1-expressing cells, CI-MPR demonstrated a paranuclear staining pattern that overlapped with TGN46 (Figure 2A). However, in PACS-1$_{GGAmut}$-expressing cells, CI-MPR showed a pronounced redistribution to an endosomal population that overlapped with the early endosomal marker EEA1. As a control, we asked whether PACS-1$_{GGAmut}$ disrupted the localization of furin, which requires PACS-1 for endosome-to-TGN retrieval (Wan *et al*, 1998), but lacks the canonical D/ExxLL GGA-binding motif (Figure 2B). We found that expression of PACS-1 or PACS-1$_{GGAmut}$ failed to affect the TGN localization of FLAG-furin, suggesting that PACS-1$_{GGAmut}$ selectively disrupts the trafficking of itinerant cargo that depend on binding to both PACS-1 and GGAs. Because GGA3 distributes between the TGN and early endosomes (Puertollano and Bonifacino, 2004), we also examined the localization of GGA3 in PACS-1$_{GGAmut}$-expressing cells (Figure 2C). We found that expression of PACS-1$_{GGAmut}$, but not PACS-1, caused a striking redistribution of GGA3 from a paranuclear localization to a dispersed endosome population that overlapped with the redistributed CI-MPR. In addition, we tested the effect of a interfereing mutant PACS-1 molecule, PACS-1$_{Admut}$, that fails to bind AP-1 and redistributes the CI-MPR and furin from the TGN (Crump *et al*, 2001), on the localization of GGA3. We observed no effect of PACS-1$_{Admut}$ expression on the localization of GGA3 (Figure 2C), suggesting that redistribution of GGA3 to endosomal compartments induced by PACS-1$_{GGAmut}$ results from the inability of PACS-1$_{GGAmut}$ to interact with GGA3. These findings suggest the PACS-1/GGA3 interaction is required for CI-MPR retrieval and for release of GGA3 from endosomal membranes.

PACS-1 is required for CI-MPR function

To better understand how PACS-1 and GGA3 might cooperate to direct trafficking of CI-MPR, we conducted protein–protein binding assays to define the PACS-1-binding site on the CI-MPR$_{CD}$. Previously, we found that truncation of the last 10 amino acids (…DDpS$_{2484}$DEDLLHI) of the CI-MPR$_{CD}$, which contain a CK2 phosphorylatable acidic cluster and constitute a DxxLL GGA-binding motif, abolished binding to the FBR region of PACS-1 (Wan *et al*, 1998). First, we sought to determine if, similar to the interaction of PACS-1 and furin (Wan *et al*, 1998), as well as the CI-MPR with GGA3 (Kato *et al*, 2002), phosphorylation of CI-MPR Ser$_{2484}$ would enhance binding to the PACS-1 FBR (Figure 3A). We tested the binding of Trx-PACS-1$_{FBR}$ to GST-CI-MPR$_{CD}$ phosphorylated by CK2 or to GST-CI-MPR$_{CD}$ mutants containing a phosphomimic Ser$_{2484}$→Asp or nonphosphorylatable Ser$_{2484}$→Ala substitution. We found that both preincubation of GST-CI-MPR$_{CD}$ with CK2 and the Ser$_{2484}$→Asp substitution enhanced binding to Trx-PACS-1$_{FBR}$, indicating that like other PACS-1 cargo proteins, CK2 phosphorylation of Ser$_{2484}$ within the CI-MPR acidic cluster enhanced binding to PACS-1. Second, we conducted an alanine scan of each of the acidic residues from Asp$_{2482}$ to Asp$_{2487}$ and found that alanine mutation of any of the acidic residues reduced binding to Trx-PACS-1$_{FBR}$ (Figure 3B). Finally, we found that Leu$_{2488}$→Ala and Leu$_{2489}$→Ala mutations had no effect on Trx-PACS-1$_{FBR}$ binding, whereas these mutations completely blocked Trx-GGA3$_{VHS-GAT}$ binding, as previously reported (Figure 3C and Puertollano *et al*, 2001a). Thus, PACS-1 and GGA3 share overlapping but not identical CI-MPR-binding sites.

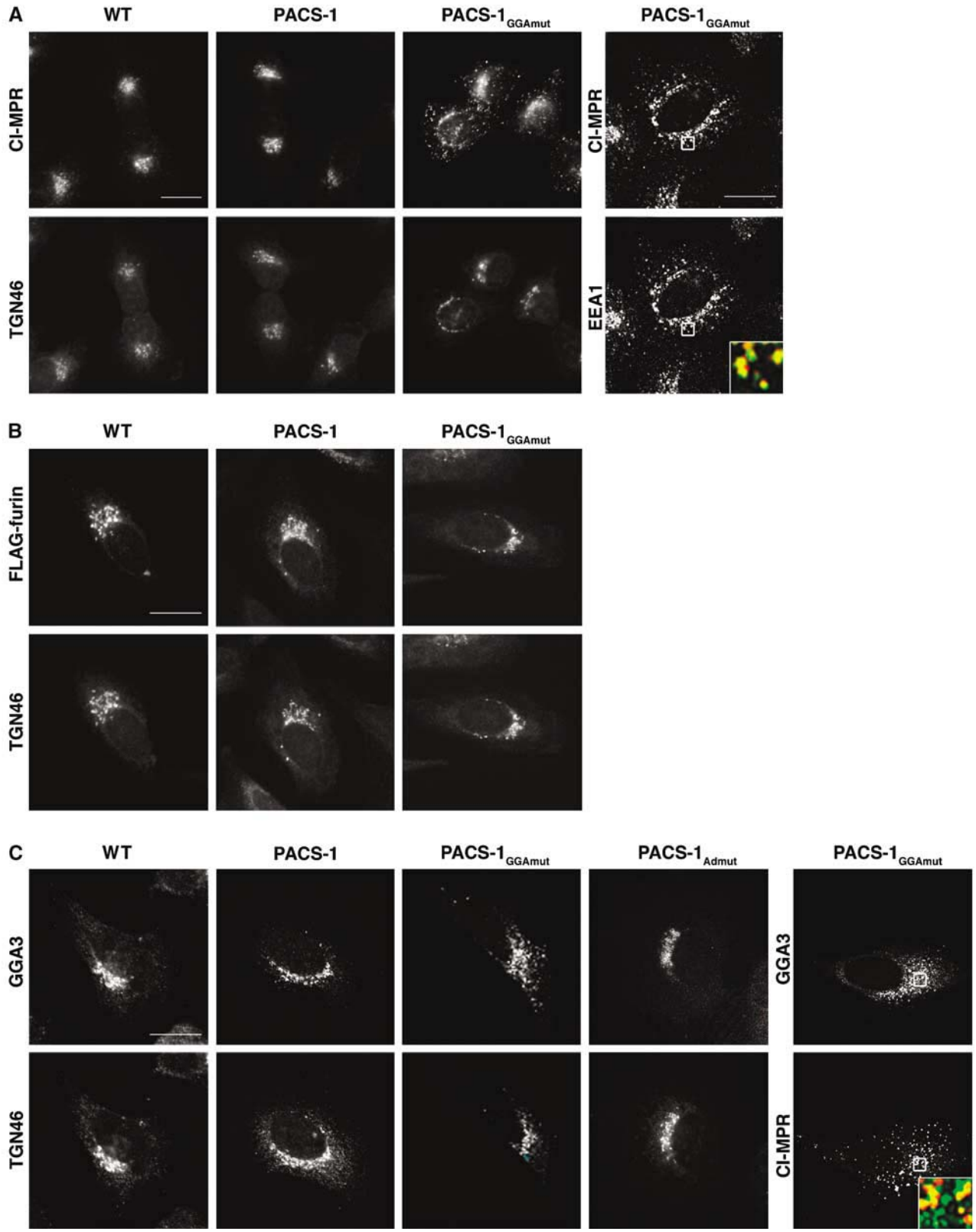

Figure 2 PACS-1_{GGAmut} disrupts CI-MPR trafficking. (**A**) A7 cells infected with WT vaccinia virus (VV) or VV recombinants expressing PACS-1 or PACS-1_{GGAmut} were stained with antibodies to detect CI-MPR, TGN46 or EEA1 as indicated. Inset: colocalization of CI-MPR (green) and EEA1 (red) from the boxed area. CI-MPR staining outside the TGN area increased from 11 ± 5 and $9 \pm 7\%$ in the WT and PACS-1-expressing cells, respectively, to $40 \pm 10\%$ for PACS-1_{GGAmut}-expressing cells. (**B**) A7 cells expressing FLAG-furin were treated as in (A) and stained with anti-FLAG and anti-TGN46. (**C**) A7 cells infected with VV:WT or with VV expressing PACS-1, PACS-1_{Admut} or PACS-1_{GGAmut} and then costained with anti-GGA3 and anti-TGN46 or anti-CI-MPR. Inset: Colocalization of GGA3 (green) and CI-MPR (red) from the boxed area. GGA3 staining outside the TGN area increased from 11 ± 6, 8 ± 4 and $9 \pm 5\%$ in the WT, PACS-1- and PACS-1_{Admut}- expressing cells, respectively, to $38 \pm 7\%$ for PACS-1_{GGAmut}-expressing cells. Scale bars = 20 μm.

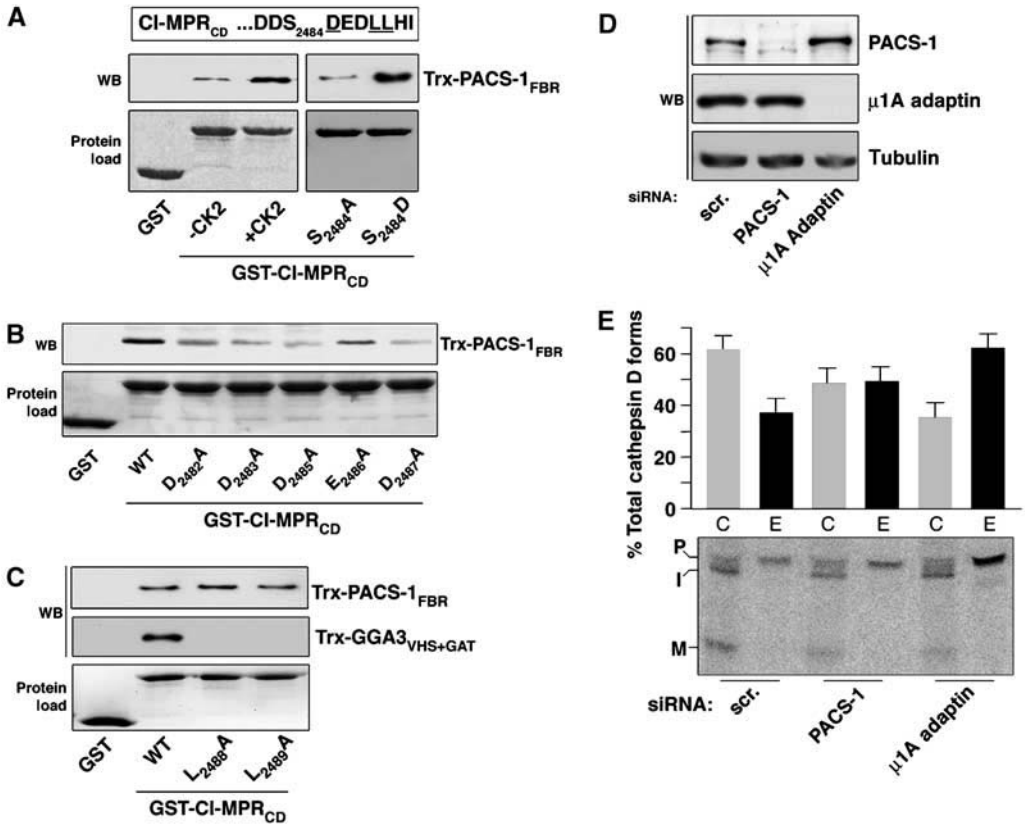

Figure 3 PACS-1 is required for CI-MPR function. (**A–C**) GST, GST-CI-MPR$_{CD}$ preincubated or not with CK2, or GST-CI-MPR$_{CD}$ containing the indicated mutations was incubated with Trx-PACS-1$_{FBR}$ (residues 117–294) or Trx-GGA3$_{VHS+GAT}$, isolated with glutathione sepharose, washed three times with GST-binding buffer containing 4% NP-40 and analyzed by Western blot using anti-Trx (upper panels). Input of each GST-protein is shown (lower panel). GST-CI-MPR$_{CD}$ pulled down ~1% of the Trx-PACS-1$_{FBR}$. (**D**) A7 cells were treated with scrambled (scr.) or PACS-1 siRNAs and cell lysates analyzed by Western blot using anti-PACS-1 or anti-tubulin. (**E**) A7 cells were treated with the indicated siRNA and Cathepsin D pulse chase experiments performed. Cellular and secreted fractions were immunoprecipitated with anti-cathepsin D and analyzed by fluorography. Precursor (P), intermediate (I) and mature (M) forms of cathepsin D are shown (lower panel). The percentage of missorted (secreted) cathepsin D compared to the processed form is shown ($n=3$, $P=0.01$).

The importance of CI-MPR Asp$_{2485}$, which is required for GGA binding and sorting of lysosomal enzymes (Chen *et al*, 1997; Puertollano *et al*, 2001a), for binding to PACS-1, as well as the requirement of PACS-1 for the TGN localization of CI-MPR (Wan *et al*, 1998; Simmen *et al*, 2005), led us to determine if PACS-1 is required for CI-MPR function. Therefore, we investigated the effect of PACS-1 depletion on the sorting of lysosomal enzymes by CI-MPR. The sorting and maturation of cathepsin D, a ligand of CI-MPR, to lysosomes was followed in metabolically labeled cells. The intracellular (C) and extracellular (E) forms of cathepsin D were immunoprecipitated from both the cells and medium after pulse-chase in the presence of mannose-6-phosphate. We found that siRNA depletion of PACS-1 (Figure 3D), which redistributes CI-MPR from the TGN (Simmen *et al*, 2005), caused an ~20% increase in secreted cathepsin D and a corresponding ~20% decrease in intracellular cathepsin D compared to control cells (Figure 3E). As a positive control, and in agreement with previous studies, we found that siRNA depletion of the μ1A subunit of AP-1 caused ~50% of the newly synthesized procathepsin D to be released into the culture medium. Additionally, we observed no change in the half-life of CI-MPR in PACS-1-depleted cells (data not shown), indicating that this increased secretion of cathepsin D does not result from decreased CI-MPR stability.

PACS-1 binds to and activates CK2

The overlapping PACS-1- and GGA3-binding sites on CI-MPR, as well as the requirement for binding of PACS-1 to GGA3 to control the TGN localization of CI-MPR, suggested that the interaction between PACS-1, GGA3 and CI-MPR is tightly regulated. One clue to the underlying mechanism controlling the PACS-1/GGA3-dependent sorting of CI-MPR is the prominent role CK2 phosphorylation plays in the regulation of each protein (Doray *et al*, 2002a; Scott *et al*, 2003). Although earlier studies demonstrated that an AP-1-associated CK2 activity could phosphorylate GGA1 (Doray *et al*, 2002b), we speculated that a more direct association of CK2 with PACS-1 and GGA3 might afford greater signaling efficacy. Accordingly, we immunoprecipitated PACS-1 from rat brain and assayed the bound material for co-precipitating CK2 activity (Figure 4A). We observed a ~14-fold increase in PACS-1-associated CK2 activity compared to the control, which was blocked by the CK2-specific inhibitor TBB, but not the PKA inhibitor PKI. To identify the region of PACS-1 that associates with CK2, we used GST-PACS-1 segments (see Figure 1A) to capture CK2α from rat brain cytosol (Figure 4B). Similar to our analysis of GGA3 binding (Figure 1), we found that CK2α was captured solely by GST-PACS-1$_{FBR}$. We more precisely identified PACS-1 FBR residues required for CK2 binding by testing a battery of

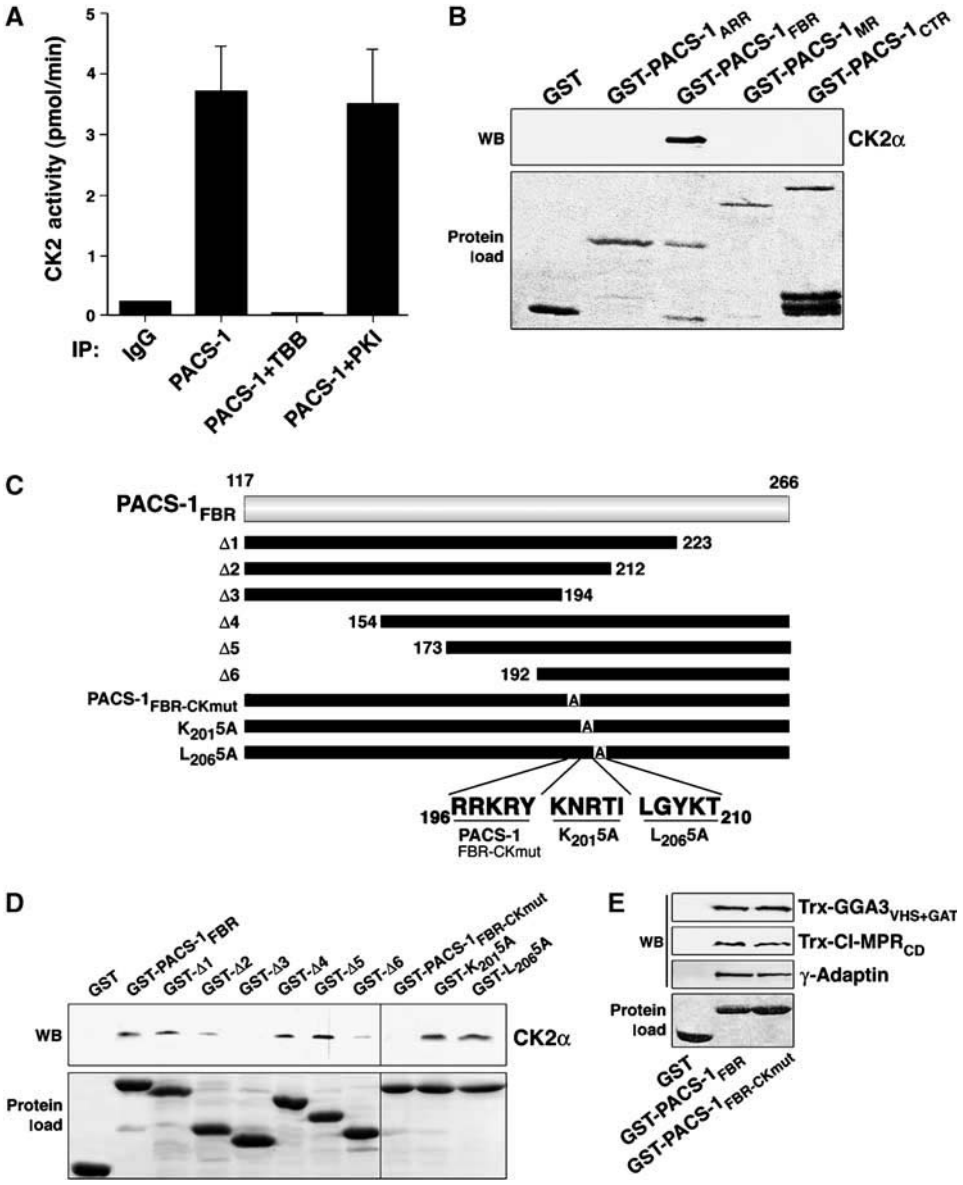

Figure 4 PACS-1 associates with CK2. (**A**) Rat brain cytosol was incubated with affinity-purified anti-PACS-1 or control IgG to immunoprecipitate endogenous PACS-1, and co-precipitating CK2 activity was measured with an *in vitro* kinase assay in the absence or presence of 40 μM TBB (CK2 inhibitor) or 400 μM PKI (PKA inhibitor). Error bars represent mean and s.d. of three independent experiments. (**B–D**) GST-PACS-1 ARR, FBR (residues 117–266), MR or CTR, or the indicated PACS-1 FBR truncations or alanine substitutions (see Figure 1A and D) were incubated with rat brain cytosol, captured with glutathione sepharose and analyzed by Western blot using anti-CK2α (panel B, D, upper panel). Input of each GST-protein is also shown (panel B, D, lower panel). GST-PACS-1_{FBR} captured ~3% of the input CK2α. Relative to GST-PACS-1_{FBR}, the interaction of CK2 with GST-Δ2 and GST-Δ6 was reduced 60 and 75%, respectively ($n = 3$). (**E**) GST, GST-PACS-1_{FBR} (residues 117–266) or GST-PACS-$1_{FBR-CKmut}$ was incubated with Trx-$GGA3_{VHS+GAT}$, Trx-CI-MPR_{CD} or purified AP-1, captured with glutathione sepharose and analyzed by Western blot using anti-Trx or anti-γ-Adaptin antibody (upper panels). GST-PACS-1_{FBR} (residues 117–266) pulled down 9% of the Trx-CI-MPR_{CD}. Input of each GST-protein is shown (lower panel).

GST-PACS-1_{FBR} truncations and substitutions for their ability to capture CK2α from rat brain cytosol (Figure 4C). We found that an 18-amino acid segment of the PACS-1 FBR between L_{194} and A_{212} was required to capture CK2α (Figure 4D). Next, we conducted an alanine scan of this PACS-1 segment and found that an R_{196}RKRY→AAAAA substitution (hereafter called PACS-$1_{FBR-CKmut}$) blocked CK2α association with GST-PACS-1_{FBR}, whereas alanine substitution of adjacent five-amino-acid segments, including K_{201}NRTI→AAAAA and L_{206}GYKT→AAAAA, did not. As a control, we observed no difference between the binding of GST-PACS-1_{FBR} or GST-PACS-$1_{FBR-CKmut}$ to purified AP-1, Trx-CI-MPR_{CD} or Trx-$GGA3_{VHS+GAT}$ (Figure 4E). Thus, PACS-1 associates with CK2 *in vivo* and the PACS-1 FBR-CKmut substitution specifically blocks the CK2/PACS-1 interaction.

To determine which CK2 subunit associates with PACS-1, we conducted a yeast-two-hybrid analysis (Figure 5A). We found that yeast expressing PACS-1 FBR and CK2β, but not CK2α or CK2α′, supported growth under histidine selection. Moreover, cotransformation of PACS-$1_{FBR-CKmut}$ with CK2β failed to support cell growth, further indicating that PACS-1 R_{196}RKRY is required for the interaction between the PACS-1 FBR and CK2β. To determine if the PACS-1 FBR binds directly to CK2β, we conducted a protein–protein binding assay, and

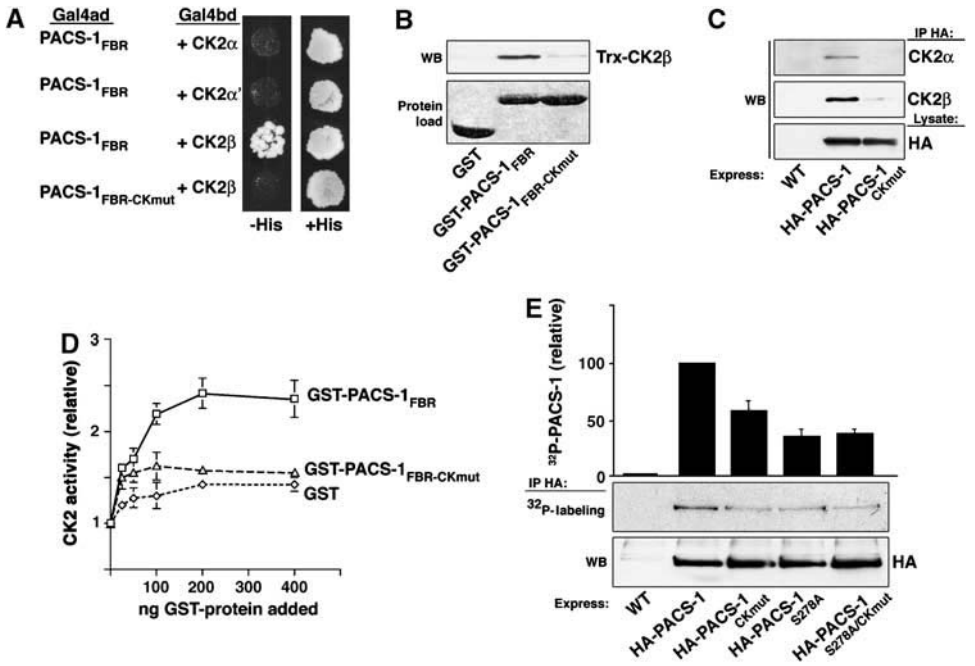

Figure 5 PACS-1 binding to CK2β activates CK2. (**A**) Yeast transformed with the indicated Gal4 activation and DNA-binding domain (Gal4ad and Gal4bd) constructs were screened for growth on His^+ and His^- media. (**B**) GST, GST-PACS-1_{FBR} (residues 117–266) or GST-PACS-$1_{FBR-CKmut}$ was incubated with Trx-CK2β, isolated with glutathione sepharose, washed twice with GST-binding buffer, once with GST-binding buffer containing 1% deoxycholate and analyzed by Western blot using anti-Trx (upper panel). Input of each GST-protein is shown (lower panel). GST-PACS-1_{FBR} captured 2.5% of the input Trx-CK2β. (**C**) A7 cells infected with VV:WT or VV expressing HA-PACS-1 or HA-PACS-1_{CKmut} were lysed, immunoprecipitated with HA antibody and any co-immunoprecipitating CK2α and CK2β detected by Western blot using subunit-specific antisera (upper panels). HA-PACS-1 expression is shown (bottom panel). (**D**) *In vitro* CK2 holoenzyme activity assayed in the absence or presence of purified GST, GST-PACS-1_{FBR} (residues 117–266) or GST-PACS-$1_{FBR-CKmut}$. Activity is normalized to a parallel sample assayed in the absence of added protein. Error bars represent mean and s.d. of three independent experiments. (**E**) A7 cells were infected with VV:WT or VV expressing HA-PACS-1, HA-PACS-1_{CKmut}, HA-PACS-1_{S278A} or HA-PACS-$1_{S278A/CKmut}$ and metabolically labeled with $^{32}P_i$. HA-proteins were immunoprecipitated with mAb HA.11, resolved by SDS–PAGE and analyzed by autoradiography (upper panel). HA-PACS-1 expression is shown (bottom panel). Error bars represent mean and s.d. of three independent experiments.

found that Trx-CK2β bound directly to GST-PACS-1_{FBR} but not GST-PACS-$1_{FBR-CKmut}$ (Figure 5B). Finally, to confirm the effect of the CKmut substitution in the context of full-length PACS-1, we expressed full-length HA-PACS-1 or HA-PACS-1_{CKmut} in cells, immunoprecipitated the PACS-1 proteins and examined co-precipitating endogenous CK2α and β by Western blot (Figure 5C). In agreement with the *in vitro* protein capture studies, we found that HA-PACS-1, but not HA-PACS-1_{CKmut}, co-precipitated CK2.

One characteristic property of CK2 is the three-fold activation observed upon binding of polycationic molecules or proteins containing clusters of basic amino acids to a patch of acidic residues in the regulatory β subunit (Bonnet *et al*, 1996; Leroy *et al*, 1997). As the R_{196}RKRY cluster of basic amino acids in the PACS-1 FBR is required for binding to CK2β, we tested the effect of PACS-1 on CK2 activity levels using an *in vitro* kinase assay. Purified bovine CK2 holoenzyme was preincubated with increasing concentrations of GST, GST-PACS-1_{FBR} or GST-PACS-$1_{FBR-CKmut}$, and CK2 activity was scored as incorporation of ^{32}P into a peptide substrate (Figure 5D). GST-PACS-1_{FBR} stimulated CK2 activity ~2.5-fold, whereas GST or GST-PACS-$1_{FBR-CKmut}$ had a lesser (~0.5-fold) effect on CK2 activity. Thus, PACS-1 FBR binding stimulates the activity of the CK2 holoenzyme.

We previously determined that CK2 phosphorylation of Ser_{278} within the PACS-1 autoregulatory domain activates cargo binding and accounts for ~50% of the incorporated phosphate on PACS-1 (Scott *et al*, 2003). Thus, our finding that PACS-1 bound and activated CK2 suggested that this interaction may be critical for regulating the phosphorylation state of PACS-1. To test this possibility, we metabolically labeled replicate plates of cells expressing full-length HA-PACS-1, HA-PACS-1_{CKmut} or HA-PACS-1_{S278A} with $^{32}P_i$, and quantified the amount of radiolabel incorporated into each protein (Figure 5E). We observed ~40% less ^{32}P incorporation into HA-PACS-1_{CKmut} compared to HA-PACS-1, whereas HA-PACS-1_{S278A} exhibited ~60% less ^{32}P incorporation compared to HA-PACS-1. This indicated that the PACS-1/CK2 interaction is required for efficient PACS-1 phosphorylation, but does not reduce PACS-1 phosphorylation to the level observed by Ser_{278}→Ala substitution. Therefore, to gauge whether the CKmut substitution affects PACS-1 Ser_{278} phosphorylation, we examined the ^{32}P incorporation into a PACS-$1_{S278A/CKmut}$ double mutant. We predicted that if CK2 that is bound to PACS-1 phosphorylates only Ser_{278}, then PACS-$1_{S278A/CKmut}$ would exhibit equal ^{32}P incorporation compared to PACS-1_{S278A}. Conversely, if CK2 bound to PACS-1 primarily phosphorylates residues other than Ser_{278}, then PACS-$1_{S278A/CKmut}$ would incorporate less ^{32}P than PACS-1_{S278A}. We observed no difference between the ^{32}P incorporation of HA-PACS-1_{S278A} and HA-PACS-$1_{S278A/CKmut}$, suggesting that CK2 binding to PACS-1 is required for efficient phosphorylation of Ser_{278} and thus the ability of PACS-1 to bind cargo.

PACS-1-bound CK2 inactivates GGA3 to retrieve CI-MPR to the TGN

The inhibitory effects of the CKmut substitution suggested that PACS-1_{CKmut} may interfere with the PACS-1-dependent sorting of membrane cargo. To test this possibility, we expressed PACS-1_{CKmut} in cells and determined any effect on the TGN localization of CI-MPR and furin. Similar to PACS-1_{GGAmut}, PACS-1_{CKmut} caused CI-MPR to redistribute to an EEA1-positive compartment (Figure 6A). We also found that PACS-1_{CKmut} caused furin to redistribute from the TGN, suggesting that PACS-1 binding to CK2 is required for the sorting of all PACS-1 cargo (Figure 6B). To determine whether PACS-1_{CKmut} blocked PACS-1-dependent trafficking solely because this mutant cannot bind CK2 to phosphorylate Ser_{278}, we expressed a double mutant, PACS-$1_{S278D/CKmut}$, in cells (Figure 6A). We previously showed that the phosphomimic construct PACS-1_{S278D} had no effect on PACS-1-dependent sorting when expressed in cells, and could rescue the disruption of endosome-to-TGN trafficking caused by depletion of PACS-1 in a cell-free assay (Scott *et al*, 2003). Therefore, based on our determination that CK2 bound to PACS-1 is required for efficient phosphorylation of Ser_{278} (Figure 5), we

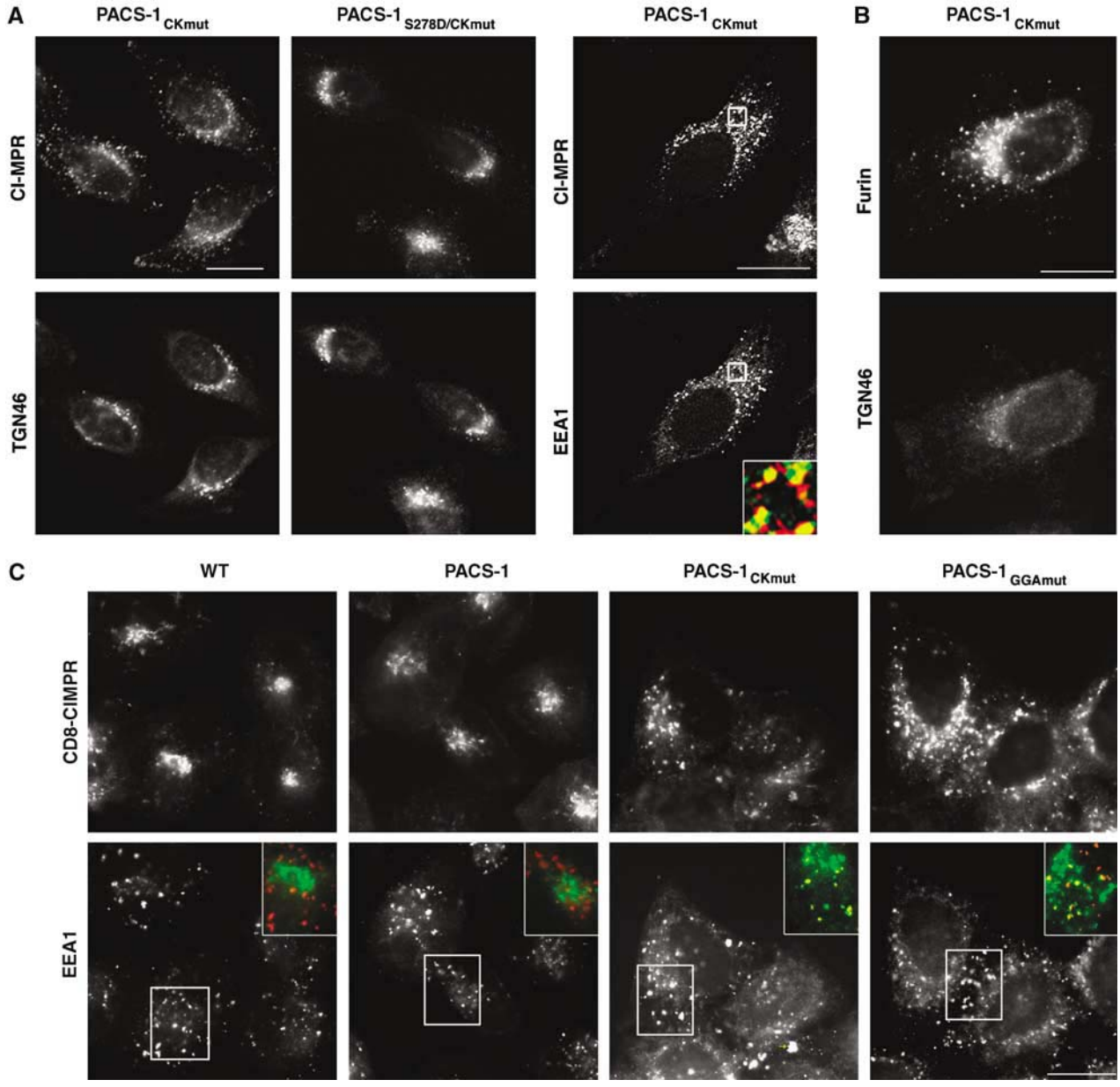

Figure 6 PACS-1_{CKmut} blocks trafficking of CI-MPR and furin. (**A**) A7 cells infected with VV expressing PACS-1_{CKmut} or PACS-$1_{CKmut/S278D}$, then stained with anti-CI-MPR, anti-TGN46 or anti-EEA1. Inset: colocalization of CI-MPR (green) and EEA1 (red). CI-MPR staining outside the TGN area was 13 ± 6 and $10 \pm 5\%$ in the WT and PACS-1-expressing cells (Figure 2A), respectively, compared with $39 \pm 9\%$ for PACS-1_{CKmut}-expressing cells and $11 \pm 7\%$ in PACS-$1_{CKmut/S278D}$-expressing cells. (**B**) A7 cells transfected with FLAG-furin, infected with VV expressing PACS-1_{CKmut} and stained with anti-FLAG and anti-TGN46. FLAG-furin staining outside the TGN area increased from 9 ± 6 and $11 \pm 4\%$ in the WT and PACS-1-expressing cells (Figure 2B), respectively, to $36 \pm 5\%$ in PACS-1_{CKmut}-expressing cells. (**C**) HeLa:CD8-CIMPR cells infected with WT VV or VV expressing PACS-1, PACS-1_{CKmut} or PACS-1_{GGAmut} were incubated with 4 μg/ml anti-CD8 for 1 h at 37°C, fixed, and then incubated with anti-EEA1 and stained with subtype-specific secondary antibodies. Inset: Staining of CD8-CIMPR (green) and EEA1 (red).

predicted that the PACS-$1_{S278D/CKmut}$ double mutant would override the disruption of CI-MPR localization caused by PACS-1_{CKmut}. Accordingly, we found that expression of PACS-$1_{S278D/CKmut}$ had no effect on the localization of CI-MPR (Figure 6A). Together, these results suggest that PACS-1 recruits CK2 and activates the kinase to promote cargo binding by phosphorylating Ser_{278} in the PACS-1 autoregulatory domain.

Next, we asked whether PACS-1_{CKmut} or PACS-1_{GGAmut} interferes with the retrieval of internalized CI-MPR to the TGN. Due to a lack of mAbs that can be used to monitor the trafficking endogenous CI-MPR following endocytosis, we chose to study the effect of the PACS-1 mutants on the trafficking of internalized CD8-CIMPR, a chimera containing the CD8 lumenal domain fused to the CI-MPR transmembrane and cytosolic domains (Seaman, 2004). Accordingly, we found that PACS-1_{Ckmut} and PACS-1_{GGAmut}, but not PACS-1, blocked the retrieval of CD8-CIMPR to the paranuclear region and caused the reporter to accumulate in an EEA1-positive compartment (Figure 6C).

The ability of PACS-1_{CKmut} and PACS-1_{GGAmut} to redistribute CI-MPR to EEA1-positive endosomes (Figure 6A and C) suggested that, as for PACS-1_{GGAmut}, PACS-1_{CKmut} might disrupt the steady-state localization of GGA3. Accordingly, we found that PACS-1_{CKmut} caused GGA3 to redistribute with CI-MPR to an endosome population (Figure 7A). Because CK2 phosphorylation of GGA3 blocks cargo binding (Doray *et al*, 2002a), we next asked whether the ability of PACS-1 to bind GGA3 may affect the efficiency of GGA3 phosphorylation by CK2. Therefore, we metabolically labeled cells expressing HA-PACS-1 or HA-PACS-1_{CKmut} with $^{32}P_i$ and quantified the amount of immunoprecipitated, ^{32}P-labeled, endogenous GGA3 (Figure 7B). We found that HA-PACS-1 expression increased the amount of ^{32}P-GGA3, whereas expression of HA-PACS-1_{CKmut} reduced by ~45% the amount of ^{32}P-GGA3. These results suggest that PACS-1 recruits CK2 to GGA3, enabling CK2 to phosphorylate and inactivate the binding of GGA3 to CI-MPR. To further test this possibility, we determined whether PACS-1 could form a ternary complex with GGA3 and CK2β *in vitro* and found that GST-$GGA3_{VHS+GAT}$ could capture Trx-CK2β only in the presence of Trx-PACS-1_{FBR} (Figure 7C). Together, our results suggest that PACS-1 recruits CK2 to phosphorylate both PACS-1 and GGA3, thereby inactivating GGA3 and activating PACS-1, thus causing PACS-1 to bind CI-MPR and direct its retrieval to the TGN.

Discussion

The results presented here show that PACS-1, GGA3 and CK2 form a multimeric complex to regulate the endosomal sorting and TGN retrieval of CI-MPR. We found that PACS-1 FBR binds directly to the cargo-binding VHS domain of GGA3 (Figure 1). Substitution of PACS-1 residues $K_{249}Y_{251}$ (PACS-1_{GGAmut}) blocked binding of PACS-1 to GGA3, but had no effect on adaptor, cargo protein or CK2 binding (Figure 1 and data not shown). Likewise, mutation of the R_{196}RKRY basic amino-acid cluster (PACS-1_{CKmut}) blocked binding of PACS-1 to CK2β, but did not affect cargo, adaptor or GGA3 binding (Figures 4 and 5). Expression of PACS-1_{GGAmut} or PACS-1_{CKmut} caused the redistribution of CI-MPR and GGA3 from the TGN to an early endosomal compartment and also blocked the

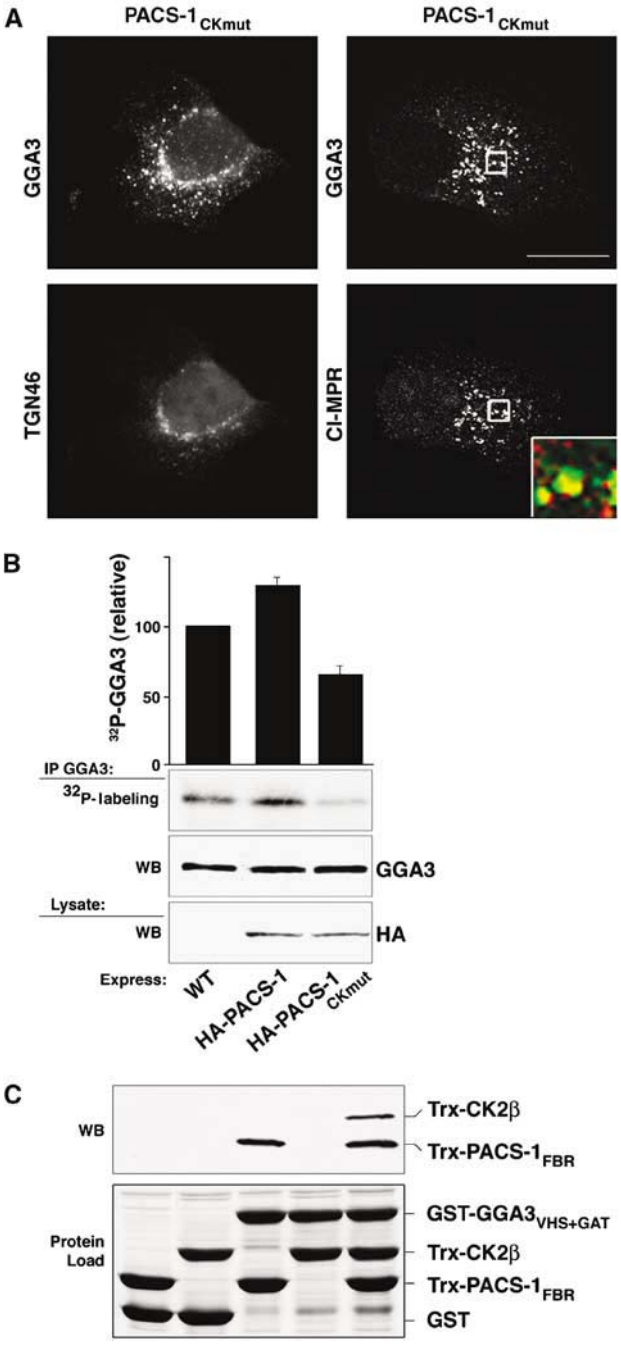

Figure 7 PACS-1_{Ckmut} redistributes GGA3 and controls GGA3 phosphorylation. (**A**) A7 cells infected with VV expressing PACS-1_{CKmut}, then stained with anti-GGA3 and anti-TGN46 or anti-CI-MPR. Inset: Colocalization of GGA3 (green) and CI-MPR (red). GGA3 staining outside the TGN area increased from 11±6 and 8±4% in the WT and PACS-1-expressing cells (Figure 2), respectively, to 36±5% in PACS-1_{CKmut}-expressing cells. Scale bars = 20 μm. (**B**) A7 cells were infected with WT:VV or VV expressing HA-PACS-1 or HA-PACS-1_{CKmut}, metabolically labeled with $^{32}P_i$, and endogenous GGA3 was immunoprecipitated and analyzed by 12% SDS–PAGE and autoradiography. Error bars represent mean and s.d. of three independent experiments normalized to the PACS-1 sample. (**C**) GST-$GGA3_{VHS+GAT}$ or GST alone was incubated with Trx-CK2β or Trx-PACS-1_{FBR} (residues 117–294) or both, isolated with glutathione sepharose using 4% NP40 and analyzed with anti-Trx mAb (upper panel). Input of each fusion protein is shown (lower panel). Trx-CK2β (~0.1%) input was captured in the GST-$GGA3_{VHS-GAT}$/Trx-PACS-1_{FBR}/CK2β ternary complex.

ability of internalized CD8-CIMPR to traffic to the TGN, causing this CI-MPR reporter to also accumulate in EEA1-positive endosomes (Figures 2 and 6). However, only PACS-1_{CKmut} disrupted TGN localization of furin (Figure 6), suggesting that the interaction of PACS-1 with GGA3 is specifically required for the trafficking of a subset of cargo proteins that bind to both PACS-1 and GGAs. Furthermore, binding of PACS-1 to CK2β stimulated CK2 activity (Figure 5), and was required for the phosphorylation of both PACS-1Ser_{278} and GGA3, which forms a ternary complex with PACS-1 and CK2β (Figures 5 and 7). Considering the known requirement for CK2 phosphorylation to regulate cargo binding of PACS-1 and GGA3 (Doray *et al*, 2002a; Scott *et al*, 2003), one interpretation of these findings is that PACS-1 directs CK2 to GGA3 to initiate the retrieval of CI-MPR from endosomes to the TGN.

Previously, we and others reported that CI-MPR requires an acidic cluster/PACS-1-dependent retrieval step to localize to the TGN (Wan *et al*, 1998), and function for lysosomal enzyme sorting (Chen *et al*, 1997). Here we show that CK2 phosphorylation of Ser_{2484}, within the CI-MPR acidic cluster, enhances binding to PACS-1, and that each of the acidic residues within the CI-MPR acidic cluster contributes to PACS-1 binding (Figure 3). By contrast, binding of PACS-1 to CI-MPR is not affected by mutation of LL_{2489}, which are required for GGA3 binding (Figure 3 and Puertollano *et al*, 2001a). Thus, PACS-1 and GGA3 bind to overlapping but distinct motifs on the CI-MPR. In addition, siRNA depletion of PACS-1 disrupted maturation and lysosomal delivery of cathepsin D, but had no effect on CI-MPR stability. These results differ from those observed with depletion of the retromer subunit Vps26 (Arighi *et al*, 2004) or TIP47 (Diaz and Pfeffer, 1998), molecules that function in retrieving CI-MPR from Hrs-coated maturing endosomal intermediates or late endosomes, respectively, to the TGN and whose depletion results in a dramatic reduction of CI-MPR half-life. This suggests that PACS-1 functions upstream of or in a separate pathway from retromer and TIP47 for sorting CI-MPR. Interestingly, the cytosolic domain of sortilin, which also sorts lysosomal cargo, binds to GGAs (Nielsen *et al*, 2001; Lefrancois *et al*, 2003) and PACS-1 (our unpublished data), and contains a cluster of acidic residues nearly identical to that found on the CI-MPR. Thus, the mechanism described here for control of CI-MPR trafficking may be common to other acidic-dileucine containing receptors. Possibly, the interaction of PACS-1 with CK2 and GGA3 prolongs movement of CI-MPR through endosomes, representing a timing mechanism to aid ligand uncoupling before retrieval of the receptor to the TGN. Alternatively, PACS-1 and GGA3 may combine to retrieve non-ligated CI-MPR to the TGN, whereas ligated receptor would continue to the prelysosomal compartment to release cargo to lysosomes and then be retrieved to the TGN by a retromer- or TIP47-based pathway. The association of PACS-1 and GGA3 with nonligated receptor in early endosomes may explain why depletion of PACS-1 or AP-1 has no effect on CI-MPR stability, whereas disruption of retromer or TIP47 decreases the CI-MPR half-life (Diaz and Pfeffer, 1998; Meyer *et al*, 2000; Arighi *et al*, 2004; Seaman, 2004).

Our observation that the R_{196}RKRY polybasic segment is required for PACS-1 to bind and activate CK2 *in vitro* and *in vivo* (Figures 4 and 5) provides a mechanism for localizing this kinase to phosphorylate regulatory sites on PACS-1 and GGA3. In particular, our demonstration that blocking CK2β binding to PACS-1 prevented activation of the CK2 holoenzyme, caused a 40% decrease in PACS-1 phosphorylation (Figure 5), and disrupted the TGN localization of CI-MPR, furin and GGA3 (Figures 6 and 7), suggests that localization of CK2 to PACS-1 is required for activation of PACS-1 cargo binding. Exactly how PACS-1 stimulates CK2 activity remains unknown, but may occur in a similar way as spermine or FGF-2, which are proposed to bind the acidic groove of CK2β, causing a conformational change in the CK2 holoenzyme that correlates with an increase in CK2 activity (Leroy *et al*, 1995, 1997; Bonnet *et al*, 1996). Additionally, our finding that PACS-1, GGA3 and CK2β form a ternary complex *in vitro* (Figure 7), and that expression of PACS-1_{CKmut} disrupted the phosphorylation and localization of GGA3 suggests that CK2 controls GGA3 phosphorylation through an interaction with PACS-1.

The disruption of CI-MPR trafficking we observed with expression of PACS-1_{GGAmut} or PACS-1_{CKmut} (Figure 6) is similar to our findings in cells lacking PACS-1 (Wan *et al*, 1998; Simmen *et al*, 2005), or expressing dominant negative PACS-1 molecules that cannot bind cargo or AP-1 (Crump *et al*, 2001; Scott *et al*, 2003), and further supports the role of PACS-1 in the endosome-to-TGN retrieval step of acidic cluster containing cargo proteins as determined using a cell-free assay (Scott *et al*, 2003). Notably, the redistributed steady-state concentration of CI-MPR and GGA3 from the TGN to an EEA1-positive compartment we observed with expression of PACS-1_{GGAmut} or PACS-1_{CKmut} is reminiscent of that observed with overexpression of Rabaptin5, which shifts the localization of endogenous GGA1 and CI-MPR to enlarged early endosomes (Mattera *et al*, 2003). However, expression of PACS-1_{Admut}, which does not bind AP-1, caused the redistribution of the CI-MPR from the TGN (Crump *et al*, 2001), but had no effect on GGA3 localization (Figure 2), suggesting a temporal ordering of molecular interactions such that PACS-1 is required downstream of GGA3 in the endosomal sorting of CI-MPR and also recruits AP-1 to retrieve this itinerant receptor to the TGN. These results suggest that PACS-1 must bind GGA3 for GGA3 to release from an early endosome compartment and that PACS-1 does not utilize GGA3 as a clathrin adaptor, rather AP-1 or -3 must also be present (Crump *et al*, 2001). We do not know how the block of PACS-1 binding to GGA3 traps GGA3 in this endosomal compartment, but it is possible that PACS-1 is required to receive the CI-MPR from GGA3 before GGA3 can release from this compartment, or perhaps PACS-1 affects the ability of GGA3 to interact with the early endosomal membrane, possibly by directing CK2 phosphorylation.

Several reports have now identified phosphorylation sites on the GGAs (Doray *et al*, 2002a; McKay and Kahn, 2004; Kametaka *et al*, 2005), including two CK2 sites thought to regulate GGA3 function: Ser_{355} of GGA1 (which corresponds to Ser_{388} in GGA3) and Ser_{372} of GGA3. Phosphorylation of GGA1 Ser_{355} promotes an intramolecular interaction of the GGA DxxLL autoregulatory domain with the cargo-binding VHS domain (Doray *et al*, 2002a), resulting in a conformational change that correlates with an inhibition of CI-MPR binding (Ghosh and Kornfeld, 2003). CK2 phosphorylation of GGA3 Ser_{372} is required for EGF-stimulated phosphorylation of GGA3 Ser_{368} by an unidentified kinase, which causes a conformational change in GGA3 that correlates with reduced association with membranes (Kametaka *et al*, 2005). Our finding that expression of PACS-1 interfering mutants that

cannot bind GGA3 or CK2, respectively, shifted the steady-state distribution of GGA3 with CI-MPR from the TGN to an EEA1-positive compartment (Figures 2 and 7) may represent the manifold effect of phosphorylation of GGA3 Ser_{272} and Ser_{388} on binding to cargo and membranes. Whether phosphorylation of PACS-1 at sites in addition to Ser_{278} control cargo and membrane association warrant further investigation. Nonetheless, our results suggest that a CK2-initiated phosphorylation cascade controls a novel cellular mechanism for regulating the dynamic movement of membrane protein traffic through the TGN/endosomal system.

Materials and methods

Cell lines and recombinant virus

A7 and HeLa:CD8-CIMPR (from M Seaman, University of Cambridge) cells were cultured as previously described (Wan *et al*, 1998). Viral recombinants were constructed using standard methods (Blagoveshchenskaya *et al*, 2002). Vaccinia virus (VV) recombinants expressing human HA-PACS-1, HA-PACS-1_{Admut} and HA-PACS-1_{S278A} were previously described (Crump *et al*, 2001; Scott *et al*, 2003). VV and adenovirus (AV) recombiants expressing HA-PACS-1_{CKmut}, HA-PACS-1_{GGAmut} HA-PACS-$1_{S278A/CKmut}$ and HA-PACS-$1_{S278D/CKmut}$ and myc-GGA3 (long form) were constructed using techniques previously described (Blagoveshchenskaya *et al*, 2002).

DNA constructs

pGEX3x plasmids expressing PACS-1 segments ARR, FBR (residues 117–266 or 117–294 as indicated in figure legends), MR and CTR, the PACS-1 FBR truncations Δ1, Δ2, Δ4, Δ5, Δ6 and pET32-PACS-1_{FBR} (residues 117–294) expressing His/thioredoxin (Trx)-fusion proteins were previously described (Crump *et al*, 2001). PGEX3x plasmids expressing PACS-1 FBR (residues 117–266 or residues 117–294 as indicated in figure legends), Δ3, K_{201}5A, L_{206}5A, GGAmut and CKmut, GST-CI-MPR_{CD} mutants and pVP16 PACS-$1_{FBR-CKmut}$ were generated by standard PCR methods and subcloned into pGEX3x or pVP16. There are no qualitative differences on binding of cargo proteins to $FBR_{117-266}$ and $FBR_{117-294}$ but binding to $FBR_{117-294}$ is quantitatively reduced as described in legends to figures. pET32-CK2β was constructed by subcloning CK2β from pGEX3x-CK2β. pGEX3x-CK2β, pGBT9-CK2α, pGBT9-CK2α′ and pGBT9-CK2β were provided by D Litchfield. PCR3.1GGA3 as well as pGEX constructs expressing the VHS, VHS + GAT, and Hinge + GAE domains of GGA3 were provided by J Bonifacino. pET32-$GGA3_{VHS+GAT}$ was subcloned from pGEX3xG-$GA3_{VHS+GAT}$ using standard techniques. pVP16-PACS-1_{FBR} and pGEX3xCI-MPR_{CD} were previously described (Wan *et al*, 1998).

Yeast-two-hybrid

HF7c yeast were transformed with pVP16-PACS-1_{FBR} (Wan *et al*, 1998) as well as pGBT9-CK2α, pGBT9-CK2α′ or pGBT9-CK2β, then grown on media lacking histidine supplemented with 1 mM 3-aminotriazole according to standard methods (Clontech).

Protein purification

pGEX or pET32-Trx vectors were transformed into BL21 (DE3) pLysS cells (Novagen). GST- or Trx-fusion proteins were purified using glutathione sepharose (Amersham-Pharmacia) or Ni-NTA-agarose (Qiagen), respectively, according to the manufacturer's protocol. Purified porcine AP-1 was provided by S Tooze. Native CK2 was purified from bovine testicles as described (Litchfield *et al*, 1990).

Metabolic labeling

A7 cells were infected with VV expressing HA-tagged PACS-1 proteins (m.o.i. = 3) for 16 h, washed and incubated with phosphate-free media for 1 h after which 0.5 mCi/ml $^{32}P_i$ (NEN) was added for 2 h. The labeled cells were washed with PBS and lysed in labeling buffer (PBS with 1% TX-100, 50 mM NaF, 80 mM β-glycerol phosphate and 0.1 μM orthovanadate). HA-PACS-1 proteins were immunoprecipitated with mAb anti-HA.11 (IgG1, Covance no. MMS-101P), separated by SDS–PAGE and analyzed by autoradiography. To label endogenous GGA3, A7 cells were infected with VV expressing HA-PACS-1 proteins (m.o.i. = 10) for 4 h, processed as above, and endogenous GGA3 was immunoprecipitated from the cell lysate using mAb anti-GGA3 (IgG1, BD no. 612310), separated by SDS–PAGE and GGA3 phosphorylation determined by autoradiography.

Co-immunoprecipitation

Endogenous PACS-1 or PACS-2 was immunoprecipitated using affinity-purified rabbit anti-PACS-1 701 (Simmen *et al*, 2005) or purified rabbit anti-PACS-1 703 (raised against PACS-1 residues KERQLSKPLSERTNSSD_{530}) or purified rabbit anti-PACS-2 834 (raised against PACS-2 residues RITKTESLVIPSTRSE_{425}) from freshly isolated rat brain. The immunoprecipitates were separated by 10% SDS–PAGE and analyzed by Western blot with mAb GGA3 (IgG1, BD no. 612310). For co-immunoprecipitation of expressed proteins, HA-PACS-1 was immunoprecipitated with mAb anti-HA.11 (IgG1, Covance no. MMS-101P), and co-immunoprecipitating proteins were analyzed by Western blot with mAb anti-myc clone9E10 (IgG1, Santa Cruz no. sc-40), mAb anti-CK2β (IgG1, Abcam no. ab15848) or rabbit anti-CK2α (Upstate no. 06–873).

Cathepsin sorting

A7 cells were treated twice with siRNA specific for PACS-1 (CUCAGUGGUCAUCGCUGUG), μ1A (AAGGCAUCAAGUAUCGGAAGA) or a control siRNA as described (Simmen *et al*, 2005). Protein expression was determined by Western blot using purified rabbit anit-PACS-1 701, rabbit anti-μ1A Adaptin (provided by L Traub) and mAb antiacetylated α-tubulin (IgG2b, Sigma no. T6793). Cathepsin D pulse-chase analysis was performed as described (Meyer *et al*, 2000). Briefly, siRNA-treated cells were labeled with ^{35}S-Met/Cys (NEN) for 0.5 h, then chased with fresh medium containing excess methionine and 10 mM M6P for 4 h. Cathepsin D was immunoprecipitated from the media and cell extract using rabbit anti-cathepsin D (DAKO no. A0561), separated by SDS–PAGE and detected by fluorography.

Kinase assays

Endogenous PACS-1 was immunoprecipitated from rat brain using affinity-purified rabbit anti-PACS-1 701, washed twice with PBS and once with kinase buffer (20 mM MOPS, pH 7.2, 25 mM β-glycerol phosphate, 5 mM EGTA, 1 mM sodium orthovanadate and 1 mM DTT). Kinase assays were performed with 200 μM CK2 substrate (RRRDDDSDDD), 100 μM ATP, 15 mM $MgCl_2$ and 5 μCi γ-^{32}P-ATP in the absence or presence of 40 nM 4,5,6,7-tetrabromo-2-azabenzimidazole (TBB; provided by L. Pinna) or 400 nM PKI (Upstate). Reactions were incubated for 10 min at 30°C, stopped with trichloroacetic acid, spotted on to P81 paper, washed with 0.75% phosphoric acid, and counted. Kinase assays to determine the activation level of CK2 were performed as above using 40 ng native bovine CK2 and increasing amounts of GST, GST-PACS-1_{FBR} (residues 117–266) or GST-PACS-$1_{FBR-CKmut}$

GST-protein-binding assays

Lysate interactions. 3 μg of each purified PACS-1 fragment was incubated with 250 μl rat brain cytosol for 2 h at 4°C, followed by incubation with glutathione agarose for 30 min. Glutathione beads were pelleted, washed with *in vitro* binding buffer (25 mM Hepes pH 7.2, 250 mM KCl, 2.5 mM MgOAc, 100 mM NaCl) and analyzed by Western blot with rabbit anti-CK2α (Upstate no. 06–873).

Direct interactions. Except where indicated, 1 μg of Trx-protein was incubated with 3 μg of GST-protein in GST-binding buffer (20 mM Tris pH 7.5, 200 mM NaCl, 1 mM $MgCl_2$, 1% NP40) for 2 h at RT, followed by incubation with glutathione agarose for 30 min. Glutathione beads were pelleted, washed three times with GST-binding buffer, and analyzed by Western blot with mAb anti-Thioredoxin (Trx; IgG1, Invitrogen no. R920–25). GST-PACS-1 pulldown of purified AP-1 was performed as described (Crump *et al*, 2001).

Ternary complex. GST-$GGA3_{VHS+GAT}$ (3 μg) was preincubated with 3 μg Trx-PACS-1_{FBR} in GST-binding buffer containing 4% NP40 for 2 h at RT, followed by the addition of 3 μg Trx-CK2β for 2 h at RT, then glutathione agarose for 30 min. Glutathione beads were pelleted by centrifugation, washed with GST-binding buffer contain-

ing 4% NP40, and analyzed by Western blotting with mAb anti-Thioredoxin (Trx; IgG1, Invitrogen no. R920–25).

Immunofluorescence microscopy

A7 cells or HeLa:CD8-CIMPR cells grown to 80% confluency were infected with VV expressing PACS-1, PACS-1_{GGAmut}, PACS-1_{CKmut}, PACS-1_{Admut} or PACS-$1_{S278D/CKmut}$ (m.o.i. = 10) or transfected with pcDNA FLAG-furin. Cells were fixed and processed for immunofluorescence as previously described (Crump *et al*, 2001). mAb anti-CI-MPR (clone 2G11, IgG2a, obtained from S Pfeffer, 1:2 (Dintzis *et al*, 1994)), mAb anti-GGA3 (IgG1, BD no. 612310, 1:50), mAb anti-EEA1 (IgG1, BD no. 610457, 1:100), mAb anti-CD8 (clone UCHT-4, IgG2a, Sigma no. C7423, 4 μg/ml for antibody uptake studies), mAb anti-FLAG tag (M1, Kodak no. IB13006, 1:300) and rabbit anti-TGN46 (Abcam no. ab16052, 1:100) were used as primary antibodies to localize antigens. As indicates in the figure legends, following incubation with species- and subtype-specific fluorescently labeled secondary antisera (Molecular Probes), images were captured at RT using a × 60 oil immersion objective on an Olympus Fluo-View FV300 confocal laser scanning microscope and processed with the NIH Image J program or a × 63 oil immersion objective on a Leica DM-RB microscope and Hamamatsu C4742-95 digital camera and processed with the scion image 1.62 program. CI-MPR, Flag-furin and GGA3 redistribution was quantified morphometrically by comparing the staining area and pixel intensity of these molecules for each construct/marker pair (25 cells from three independent experiments), relative to the corresponding TGN stain (TGN46), according to the following formula: $(\text{Mean pixel intensity})_O \times \text{Area}_O / (\text{Mean pixel intensity})_T \times \text{Area}_T$, where O = outside the TGN and T = whole cell. Background was set to the spurious signal intensity observed in the nuclear area. Quantification of immunofluorescence images was carried out using NIH Image J. Values for each morphometric analysis are provided in the respective figure legend. Antibody uptake experiments were conducted as described previously (Scott *et al*, 2003).

Acknowledgements

We thank Q Justmann for preliminary experiments and members of the Thomas lab, C Enns, J Bonifacino and S Kaech Petrie (CROET Imaging Center) for helpful discussions. We thank J Bonifacino, D Litchfield, S Tooze, S Pfeffer, L Pinna, M Seaman and L Traub for reagents. The authors declare no financial conflict of interest with the described work. This work was supported by NIH grants AI49793 and DK37274 (to GT).

References

Arighi CN, Hartnell LM, Aguilar RC, Haft CR, Bonifacino JS (2004) Role of the mammalian retromer in sorting of the cation-independent mannose 6-phosphate receptor. *J Cell Biol* **165:** 123–133

Blagoveshchenskaya AD, Thomas L, Fellciangell SF, Hung CH, Thomas G (2002) HIV-1 Nef downregulates MHC-I by a PACS-1- and PI3K-regulated ARF6 endocytic pathway. *Cell* **111:** 853–866

Bonifacino JS (2004) The GGA proteins: adaptors on the move. *Nat Rev Mol Cell Biol* **5:** 23–32

Bonnet H, Filhol O, Truchet I, Brethenou P, Cochet C, Amalric F, Bouche G (1996) Fibroblast growth factor-2 binds to the regulatory beta subunit of CK2 and directly stimulates CK2 activity toward nucleolin. *J Biol Chem* **271:** 24781–24787

Chen HJ, Yuan J, Lobel P (1997) Systematic mutational analysis of the cation-independent mannose 6-phosphate/insulin-like growth factor II receptor cytoplasmic domain. An acidic cluster containing a key aspartate is important for function in lysosomal enzyme sorting. *J Biol Chem* **272:** 7003–7012

Crump CM, Hung CH, Thomas L, Wan L, Thomas G (2003) Role of PACS-1 in trafficking of human cytomegalovirus glycoprotein B and virus production. *J Virol* **77:** 11105–11113

Crump CM, Xiang Y, Thomas L, Gu F, Austin C, Tooze SA, Thomas G (2001) PACS-1 binding to adaptors is required for acidic cluster motif-mediated protein traffic. *EMBO J* **20:** 2191–2201

Diaz E, Pfeffer SR (1998) TIP47: a cargo selection device for mannose 6-phosphate receptor trafficking. *Cell* **93:** 433–443

Dintzis SM, Velculescu VE, Pfeffer SR (1994) Receptor extracellular domains may contain trafficking information. Studies of the 300-kDa mannose 6-phosphate receptor. *J Biol Chem* **269:** 12159–12166

Doray B, Bruns K, Ghosh P, Kornfeld SA (2002a) Autoinhibition of the ligand-binding site of GGA1/3 VHS domains by an internal acidic cluster-dileucine motif. *Proc Natl Acad Sci USA* **99:** 8072–8077

Doray B, Ghosh P, Griffith J, Geuze HJ, Kornfeld S (2002b) Cooperation of GGAs and AP-1 in packaging MPRs at the trans-Golgi network. *Science* **297:** 1700–1703

Ghosh P, Griffith J, Geuze HJ, Kornfeld S (2003) Mammalian GGAs act together to sort mannose 6-phosphate receptors. *J Cell Biol* **163:** 755–766

Ghosh P, Kornfeld S (2003) Phosphorylation-induced conformational changes regulate GGAs 1 and 3 function at the *trans*-Golgi network. *J Biol Chem* **278:** 14543–14549

Hinners I, Wendler F, Fei H, Thomas L, Thomas G, Tooze SA (2003) AP-1 recruitment to VAMP4 is modulated by phosphorylation-dependent binding of PACS-1. *EMBO Rep* **4:** 1182–1189

Kametaka S, Mattera R, Bonifacino JS (2005) Epidermal growth factor-dependent phosphorylation of the GGA3 adaptor protein regulates its recruitment to membranes. *Mol Cell Biol* **25:** 7988–8000

Kato Y, Misra S, Puertollano R, Hurley JH, Bonifacino JS (2002) Phosphoregulation of sorting signal-VHS domain interactions by a direct electrostatic mechanism. *Nat Struct Biol* **9:** 532–536

Köttgen M, Benzing T, Simmen T, Tauber R, Buchholz B, Feliciangeli S, Huber TB, Schermer B, Kramer-Zucker A, Hèopker K, Simmen KC, Tschucke CC, Sandford R, Kim E, Thomas G, Walz G (2005) Trafficking of TRPP2 by PACS proteins represents a novel mechanism of ion channel regulation. *EMBO J* **24:** 705–716

Lefrancois S, Zeng J, Hassan AJ, Canuel M, Morales CR (2003) The lysosomal trafficking of sphingolipid activator proteins (SAPs) is mediated by sortilin. *EMBO J* **22:** 6430–6437

Leroy D, Herichâe JK, Filhol O, Chambaz EM, Cochet C (1997) Binding of polyamines to an autonomous domain of the regulatory subunit of protein kinase CK2 induces a conformational change in the holoenzyme. A proposed role for the kinase stimulation. *J Biol Chem* **272:** 20820–20827

Leroy D, Schmid N, Behr JP, Filhol O, Pares S, Garin J, Bourgarit JJ, Chambaz EM, Cochet C (1995) Direct identification of a polyamine binding domain on the regulatory subunit of the protein kinase casein kinase 2 by photoaffinity labeling. *J Biol Chem* **270:** 17400–17406

Litchfield DW (2003) Protein kinase CK2: structure, regulation and role in cellular decisions of life and death. *Biochem J* **369:** 1–15

Litchfield DW, Lozeman FJ, Piening C, Sommercorn J, Takio K, Walsh KA, Krebs EG (1990) Subunit structure of casein kinase II from bovine testis. Demonstration that the alpha and alpha' subunits are distinct polypeptides. *J Biol Chem* **265:** 7638–7644

Mattera R, Arighi CN, Lodge R, Zerial M, Bonifacino JS (2003) Divalent interaction of the GGAs with the Rabaptin-5-Rabex-5 complex. *EMBO J* **22:** 78–88

McKay MM, Kahn RA (2004) Multiple phosphorylation events regulate the subcellular localization of GGA1. *Traffic* **5:** 102–116

Meggio F, Pinna LA (2003) One-thousand-and-one substrates of protein kinase CK2? *FASEB J* **17:** 349–368

Meyer C, Zizioli D, Lausmann S, Eskelinen EL, Hamann J, Saftig P, von Figura K, Schu P (2000) mu1A-adaptin-deficient mice: lethality, loss of AP-1 binding and rerouting of mannose 6-phosphate receptors. *EMBO J* **19:** 2193–2203

Nielsen MS, Madsen P, Christensen EI, Nykjaer A, Gliemann J, Kasper D, Pohlmann R, Petersen CM (2001) The sortilin cytoplasmic tail conveys Golgi–endosome transport and binds the VHS domain of the GGA2 sorting protein. *EMBO J* **20:** 2180–2190

Piguet V, Wan L, Borel C, Mangasarian A, Demaurex N, Thomas G, Trono D (2000) HIV-1 Nef protein binds to the cellular protein PACS-1 to downregulate class I major histocompatibility complexes. *Nat Cell Biol* **2:** 163–167

Puertollano R, Aguilar RC, Gorshkova I, Crouch RJ, Bonifacino JS, Cell B (2001a) Sorting of mannose 6-phosphate receptors mediated by the GGAs. *Science* **292:** 1712–1716

Puertollano R, Bonifacino JS (2004) Interactions of GGA3 with the ubiquitin sorting machinery. *Nat Cell Biol* **6:** 244–251

Puertollano R, Randazzo PA, Presley JF, Hartnell LM, Bonifacino JS (2001b) The GGAs promote ARF-dependent recruitment of clathrin to the TGN. *Cell* **105:** 93–102

Robinson MS (2004) Adaptable adaptors for coated vesicles. *Trends Cell Biol* **14:** 167–174

Saint-Pol A, Yâelamos B, Amessou M, Mills IG, Dugast M, Tenza D, Schu P, Antony C, McMahon HT, Lamaze C, Johannes L (2004) Clathrin adaptor epsinR is required for retrograde sorting on early endosomal membranes. *Dev Cell* **6:** 525–538

Scott GK, Gu F, Crump CM, Thomas L, Wan L, Xiang Y, Thomas G (2003) The phosphorylation state of an autoregulatory domain controls PACS-1-directed protein traffic. *EMBO J* **22:** 6234–6244

Seaman MN (2004) Cargo-selective endosomal sorting for retrieval to the Golgi requires retromer. *J Cell Biol* **165:** 111–122

Simmen T, Aslan JE, Blagoveshchenskaya AD, Thomas L, Wan L, Xiang Y, Feliciangeli SF, Hung CH, Crump CM, Thomas G (2005) PACS-2 controls endoplasmic reticulum-mitochondria communication and Bid-mediated apoptosis. *EMBO J* **24:** 717–729

Thomas G (2002) Furin at the cutting edge: from protein traffic to embryogenesis and disease. *Nat Rev Mol Cell Biol* **3:** 753–766

Wan L, Molloy SS, Thomas L, Liu G, Xiang Y, Rybak SL, Thomas G (1998) PACS-1 defines a novel gene family of cytosolic sorting proteins required for *trans*-Golgi network localization. *Cell* **94:** 205–216

Xiang Y, Molloy SS, Thomas L, Thomas G (2000) The PC6B cytoplasmic domain contains two acidic clusters that direct sorting to distinct trans-Golgi network/endosomal compartments. *Mol Biol Cell* **11:** 1257–1273